OsmiR530 acts downstream of OsPIL15 to regulate grain yield in rice

Wei Sun[1]* iD, Xiao Hui Xu[2]* iD, Yaping Li[1] iD, Lixia Xie[1] iD, Yanan He[1] iD, Wen Li[1] iD, Xingbo Lu[2] iD, Hongwei Sun[2] iD and Xianzhi Xie[1] iD

[1]Shandong Rice Engineering Technology Research Center, Shandong Rice Research Institute, Shandong Academy of Agricultural Sciences, Jinan 250100, China; [2]Shandong Key Laboratory of Plant Virology, Institute of Plant Protection, Shandong Academy of Agricultural Sciences, Jinan 250100, China

Summary

- MicroRNAs (miRNAs) are a class of small noncoding RNAs that play important roles in plant growth and development as well as in stress responses. However, little is known about their regulatory functions affecting rice grain yield.
- We functionally characterized a novel miRNA in rice, OsmiR530, its target *OsPL3*, and its upstream regulator phytochrome-interacting factor-like 15 (OsPIL15). Their effects on rice yield were dissected comprehensively.
- We determined that OsmiR530 negatively regulates grain yield. Blocking OsmiR530 increases grain yield, whereas OsmiR530 overexpression significantly decreases grain size and panicle branching, leading to yield loss. Additionally, *OsPL3*, which encodes a PLUS3 domain-containing protein, is targeted directly by OsmiR530. Knocking out *OsPL3* decreases the grain yield. In-depth analyses indicated that OsPIL15 activates *OsMIR530* expression by directly binding to the G-box elements in the promoter. Analyses of genetic variations suggested that the *OsMIR530* locus has likely been subjected to artificial selection during rice breeding.
- The results presented herein reveal a novel OsPIL15–OsmiR530 module controlling rice grain yield, thus providing researchers with a new target for the breeding of high-yielding rice.

Introduction

Rice (*Oryza sativa*), a model monocotyledonous plant species, is the staple food for most of the global population. Consequently, breeding high-yielding rice varieties is urgently required to cope with food shortages worldwide. The number of panicles per plant, number of effective grains per panicle, grain weight and seed-setting rate are generally considered to be the decisive factors affecting rice yield. Recent studies have revealed that several genes involved in transcriptional regulation and hormone signal transduction are important for regulating rice yield, such as Growth-regulating factor (*OsGRF4* (Duan *et al.*, 2015), *OsGRF6* (Gao *et al.*, 2015)), SOUAMOSA promoter binding protein-like (*OsSPL13* (Si *et al.*, 2016), *OsSPL16* (Wang *et al.*, 2015)), MADS-domain transcription factor (*OsMADS1*, Liu *et al.*, 2018) and GAGA-binding protein 3 (*OsGBP3*; Gong *et al.*, 2018). However, the molecular mechanisms underlying the rice yield regulatory network remain elusive.

Phytochrome-interacting factors (PIFs) form a class of basic helix-loop-helix transcription factors influencing a series of biological processes by regulating the expression of their target genes which contain G-box and/or PIF-binding E-box elements (Hornitschek *et al.*, 2012; Y. Zhang *et al.*, 2013). During the past

20 yr, PIF functions have been well-studied in the model plant *Arabidopsis thaliana*, including their effects on phytochrome-mediated photomorphogenesis, hormone signaling, and responses to biotic and abiotic stresses (Leivar & Quail, 2011; Oh *et al.*, 2012; Quint *et al.*, 2016; Paik *et al.*, 2017; Shor *et al.*, 2017). The rice genome contains six phytochrome-interacting factor-like genes (*OsPILs*), designated as *OsPIL11* to *OsPIL16* (Nakamura *et al.*, 2007). Compared with the *Arabidopsis* PIFs, there is relatively little available information regarding rice PIF functions related to growth and development, especially in terms of rice yield regulation. A recent study revealed that one of the rice PIL genes, *OsPIL15*, negatively regulates grain size (Ji *et al.*, 2019). Thus, OsPILs may contribute to unique signaling networks associated with rice seed development.

MicroRNAs (miRNAs) are a class of short noncoding RNAs that regulate the expression of target genes, with important implications for plant development and stress responses (Bartel, 2004). To date, only a few miRNAs, including OsmiR156 (Jiao *et al.*, 2010), OsmiR397 (Y. C. Zhang *et al.*, 2013), OsmiR396 (Duan *et al.*, 2015; Gao *et al.*, 2015) and miR408 (Zhang *et al.*, 2017), have been confirmed as important regulators of rice yield via their effects on grain size or panicle architecture. We previously determined that a miRNA, OsmiR530-5p_R+1 (OsmiR530), is significantly more abundant in the *phytochrome B* (*phyB*) mutant than in the wild-type (WT) control (Sun *et al.*, 2015). To

elucidate its roles in rice growth and development, we generated transgenic lines overexpressing OsmiR530 (miR530-OE) or the OsmiR530 target mimic (MIM530). Functional analyses revealed that OsmiR530 negatively regulates rice yield by altering the grain size and panicle architecture. Subsequent experiments demonstrated that OsmiR530 functions directly downstream of OsPIL15. Our results establish a new OsPIL15–OsmiR530 signaling pathway that regulates rice yield.

Materials and Methods

Plant materials and growth conditions

All of the rice plants used in this study were *Oryza sativa* L. cv Nipponbare (Nip). The *phyB* mutant and phytochrome-interacting factor-like gene (OsPIL)15-overexpressing (*PIL15*-OE) transgenic lines have been described previously (Takano *et al.*, 2005; Zhou *et al.*, 2014).

Seeds were surface-sterilized in 70% (v/v) ethanol for 30 s and then in 5% NaClO (v/v) for 20 min, after which they were rinsed six times in sterile double-distilled water. Seeds were incubated in darkness at 28°C for 3 d to induce germination.

In order to analyze the agronomic traits of the transgenic plants, we sowed seeds in mid-May. The resulting seedlings were transplanted to an irrigated field in Jinan, China (lat 36°40′N, long 117°00′E) in late June. The plants were grown in the field with routine management practices. The following agronomic traits were measured before seeds were harvested: plant height, number of primary and secondary branches, seed-setting rate and number of effective grains per main panicle. The grain length and width were measured when the seeds were harvested. For each line, *c.* 20 plants were used for statistical analyses.

Generation of transgenic rice plants

In order to generate the microRNA OsmiR530-overexpression construct, the genomic DNA sequence surrounding the pre-miR530 was amplified by PCR. The amplicon was sequenced and subcloned into the *Bam*HI and *Spe*I sites downstream of the *Ubi* promoter in the p1390-Ubi vector (Li *et al.*, 2011). To prepare the OsmiR530 target mimic construct, a 24-nucleotide motif complementary to the miR399 in *IPS1* (Franco-Zorrilla *et al.*, 2007) was replaced with a sequence complementary to miR530. The *IPS1* fragment with the miR530-complementary motif was inserted into the pENTR/D-TOPO vector (Invitrogen) and then transferred to the destination vector PC186 via LR Clonase reactions (Thermo Fisher Scientific, Waltham, MA, USA). The *OsPIL15*-overexpressing (*PIL15*-OE) transgenic plants were generated in our laboratory during a previous study (Zhou *et al.*, 2014). For the *OsPIL15-eGFP* construct, the full-length *eGFP* cDNA was amplified by PCR and then inserted at the *Bst*ÆII restriction site of the *PIL15*-OE vector (Zhou *et al.*, 2014) (GFP, green fluorescent protein). To construct the *PHYB-GFP* vector, the rice *PHYB* cDNA sequence was amplified by PCR with a nucleotide substitution that replaced the *PHYB* translation termination codon (TAG) with an oligonucleotide sequence containing a *Kpn*I site. The PHYB

moiety encoded in the *Arabidopsis PHYB-GFP* fusion construct (Yamaguchi *et al.*, 1999) was replaced with rice *PHYB* to obtain the *PHYB-GFP* construct in which the rice *PHYB-GFP* fusion sequence was inserted between the constitutive *cauliflower mosaic virus* 35S promoter and the Nos terminator. The PLUS3 domain containing protein (*OsPL3*)-knockout (*PL3*-KO) and *OsPIL15*-knockout (*PIL15*-KO) lines were generated by the Biogle company (Hangzhou, China) using CRISPR/Cas9 technology. We designed two single-guide RNAs (sgRNAs) targeting *OsPL3* (sg1: 5′-GTGAAGCCAACGGATTGCAG-3′; sg2: 5′-GCCCAGTGTT AGCCTGTTGG-3′), and two sgRNAs targeting *OsPIL15* (sg3679: 5′-GACCACCAGGGAACCCTCCA-3′; sg3680: 5′-GGAGTCGACGGTCGTGCAGA-3′) to minimize the off-target effects. All sgRNAs were generated in the BGK03 vector, which contains the *Cas9* gene. All constructs were introduced into *Agrobacterium tumefaciens* strain EHA105 cells for the subsequent transformation of Nip rice plants as described previously (Toki *et al.*, 2006). The homozygous T_3 generation plants were used for a phenotypic analysis. Details regarding the primers used for constructing vectors are provided in Supporting Information Table S1.

Field plot analysis

For the field plot experiment, the WT, miR530-OE and MIM530 plants were grown under natural conditions in Jinan, China (lat 36°40′N, long 117°00′E) in 2018. Each plot was 3 m² and comprised a mixture of three transgenic lines, except for the WT plots, with a planting density of 20 cm × 25 cm. The miR530-OE plots included miR530-OE #a1, #b5 and #c2 transgenic plants, whereas the MIM530 plots consisted of MIM530 #2, #3 and #6 transgenic plants. Plot yields were determined when the seeds were harvested. The field trial was completed according to a randomized complete block design with four replicates. Data are presented herein as the mean ± SD.

Histological analysis

Internodes just below the neck node and young spikelet hulls were fixed in 4% (w/v) glutaraldehyde for ≥ 16 h. The samples were dehydrated with a series of increasing ethanol concentrations, and then embedded in Paraplast Plus (Sigma). After preparing 8-µm sections, the samples were counter-stained and observed with the BX53 microscope (Olympus, Tokyo, Japan). For scanning electron microscopy (SEM), the lemmas from mature seeds were fixed in 2.5% (w/v) glutaraldehyde. After dehydrating with a series of increasing ethanol concentrations, the samples were dried to a critical point and mounted on stubs. The inner surfaces of the lemmas were observed with the S-3000N scanning electron microscope (Hitachi High-Technologies Corp., Tokyo, Japan). The cell length, width and area were measured with the IMAGEJ program (US National Institutes of Health, Bethesda, MD, USA).

Quantitative real-time (qRT)-PCR analysis

Total RNA (including miRNA) was extracted using the miRNeasy Mini kit (Qiagen). Residual genomic DNA was

eliminated with RNase-free DNase I (Promega). To analyze miR530 expression, miRNA first-strand cDNA was synthesized with the miRcute miRNA First-Strand cDNA Synthesis kit (Tiangen, Beijing, China). The expression of miR530 was then quantified by qRT-PCR with the SYBR PrimeScript™ miRNA RT-PCR kit (Tiangen) with 5.8S rRNA as the internal control. To analyze the expression of the OsmiR530 precursor, the target mimic and *OsPL3*, *c.* 2 µg total RNA for each sample was reverse-transcribed with the M-MLV RTase cDNA synthesis kit (TaKaRa, Dalian, China). The resulting cDNA was used as the template for a qRT-PCR assay, which was completed with the SYBR Green PCR master mix (TaKaRa). The *OsEF-1α* gene was used as the internal control. The qRT-PCR analysis involved three biological replicates for each miRNA and gene. The relative expression ratios of OsmiR530, its precursor *OsMIR530* and *OsPL3* were calculated according to the delta-delta threshold cycle relative quantification method. Details regarding the qRT-PCR primers are provided in Table S1.

In situ hybridization

The miRNA *in situ* hybridization was completed as described previously (Y. C. Zhang *et al.*, 2013). Digoxigenin-labeled antisense (5′-AGTGTTAGCCTGTTGGCGGTGTAA-3′) and sense (5′-TTACACCGCCAACAGGCTAACACT-3′) probes for *OsPL3* were synthesized by Beijing AuGCT Biotech Company, China. The 5′- and 3′-digoxin-labeled LNA™ probe for OsmiR530 (5DiGN/TAGGTGCAGGTGCAAATGCA/3DiG_N) was purchased from Qiagen (http://www.exiqon.com). A scrambled miRNA probe was used as a negative control.

RNA ligase-mediated 5′-rapid amplification of cDNA ends (RLM 5′-RACE)

The RLM 5′-RACE assay was performed with the RLM-RACE kit (Takara) according to the manufacturer's instruction. Approximately 2 µg WT seedling total RNA was ligated to the RNA Oligo adaptor without a calf intestinal phosphatase treatment. Two rounds of nested PCR were performed, after which the PCR products were inserted into a cloning vector for sequencing. The primers used in this assay are listed in Table S1.

Subcellular localization

In order to generate the *35S::OsPL3-GFP* plasmid, the full-length *OsPL3* coding sequence without the stop codon was inserted into the Cam35S-GFP vector between the *Bam*HI and *Xba*I sites. Rice protoplasts were transformed with the *35S::OsPL3-GFP* construct as described previously (Zhang *et al.*, 2012). GFP signals were observed with the FV10-ASW confocal microscope (Olympus). The far-red fluorescent protein mKate with an N-terminal nuclear localization sequence (NLS), NLS-mKate, was used for an analysis of the co-localization. The primers used in this assay are listed in Table S1.

Yeast-one-hybrid assay (Y1H)

A Y1H assay was completed with the Matchmaker™ Gold Yeast One-Hybrid Library Screening System (Clontech Laboratories, Mountain View, CA, USA). Two DNA fragments containing two adjacent G-box (5′-CACGTG-3′) and one normal G-box element in the *OsMIR530* promoter were synthesized separately (Table S1) and inserted into the reporter vector pAbAi to obtain the pMIR530A-AbAi and pMIR530B-AbAi plasmids, respectively. To test the specificity of the binding sites, two fragments carrying the same flanking regions but with mutated G-box elements (i.e. replaced with 5′-TGACCT-3′) (Table S1), were synthesized and inserted into the pAbAi reporter vector to generate the pMIR530Am-AbAi and pMIR530Bm-AbAi plasmids. The full-length *OsPIL15* coding sequence was amplified by PCR and inserted into the pGADT7 vector. The recombinant pGADT7-OsPIL15 plasmid was used to transform Y1HGold yeast strain cells carrying the linearized pMIR530A-AbAi, pMIR530B-AbAi, pMIR530Am-AbAi and pMIR530Bm-AbAi. Transformed yeast cells were detected by spotting serial dilutions (1 : 1, 1 : 10, 1 : 100 and 1 : 1000) of yeast onto agar-solidified synthetic dextrose (SD)/−Leu medium supplemented with 600 ng ml^{-1} aureobasidin A (AbA). The pGADT7-Rec-p53 and p53-AbAi plasmids were used as positive controls. Details regarding the primers used for this assay are listed in Table S1.

Electrophoretic mobility shift assay (EMSA)

An EMSA was conducted as described previously (Ma *et al.*, 2009). The full-length *OsPIL15* coding sequence was synthesized and cloned into the expression vector pET28a. The resulting recombinant plasmid was transformed into *Escherichia coli* BL21 (DE3) cells to obtain positive clones. The His-tagged fusion proteins produced in the transformed *E. coli* cells were purified as described previously (Ji *et al.*, 2019).

The G-box oligonucleotide sequences were synthesized and separately labeled with biotin by using the Biotin 3′ End DNA Labeling Kit (Beyotime, Shanghai, China). DNA probes were obtained by annealing two complementary oligonucleotides (Table S1), and then used in the assay completed with the EMSA kit (Beyotime).

Chromatin immunoprecipitation and qRT-PCR (ChIP-qPCR) analysis

A ChIP-qPCR assay was performed as described previously (Lee *et al.*, 2007). Briefly, the aboveground parts of *OsPIL15:eGFP* transgenic plants at the four-leaf stage were treated with 1% formaldehyde (i.e. cross-linking treatment). The chromatin complexes were sonicated at 4°C to generate 200–500-bp fragments. The sheared chromatin was immunoprecipitated, washed and reverse cross-linked. A polyclonal anti-GFP antibody (Abcam, Cambridge, UK) was used, with IgG as a negative control. The purified precipitated DNA was dissolved in water for a qRT-PCR analysis. Details regarding the primers used for this assay are listed in Table S1.

Transcriptional activity assay

The transcriptional activity in *Nicotiana benthamiana* leaves was examined as described previously (Sun *et al.*, 2012). The 2-kb *OsMIR530* promoter sequence was ligated to the luciferase reporter gene *LUC* in the plant binary vector pGWB35 (Nakagawa *et al.*, 2007) via Gateway reactions (Invitrogen) to generate the reporter construct. To prepare the effector construct, the *OsPIL15* coding sequence was cloned into the pCAMBIA 1300-FLAG vector between the *Bam*HI and *Spe*I restriction sites. The reporter and effector constructs were inserted separately into *A. tumefaciens* strain GV3101 cells for the subsequent co-infiltration of *N. Benthamiana* leaves. The LUC signals were detected and quantified with the NightSHADE LB 985 Plant Imaging System (Berthold, Bad Wildbad, Germany) at 48 h after infiltrations. Ten independent *N. benthamiana* leaves were infiltrated and analyzed for each of three biological replicates. Details regarding the primers used for this assay are listed in Table S1.

Yeast-two-hybrid (Y2H) assay

The GAL4-AD and GAL4-BD derivatives were generated by fusing the full-length *OsPIL15* coding sequence and the C-terminal of *PHYB* sequence (i.e. 1891–3513 bp), respectively. The AD-*OsPIL15* and BD-*PHYB*-C constructs were used to co-transform the *Saccharomyces cerevisiae* strain AH109 cells. The transformed yeast colonies were transferred to agar-solidified SD/−Leu/−Trp/−His medium to detect interactions. Details regarding the primers used for this assay are listed in Table S1.

Firefly luciferase complementation imaging (LCI) assay

An LCI assay was performed in *N. benthamiana* leaves as described previously (Sun *et al.*, 2013). The full-length *PHYB* and *OsPIL15* coding sequences were separately fused to the fragments encoding the N-terminal and C-terminal parts of *LUC*. The *N. benthamiana* leaves were co-infiltrated with the *A. tumefaciens* cells harboring the nLUC and cLUC constructs. After 48 h, the leaves were analyzed for LUC activity. The primers used in this assay are listed in Table S1.

Semi-*in vivo* pull-down assay

In order to determine the interaction between PHYB and OsPIL15, leaves were collected from WT and *PHYB-GFP* seedlings incubated for 14 d in a growth chamber with a 12-h light (28°C) : 12-h dark (24°C) cycle. Total proteins were extracted from the leaves with lysis buffer 50 mM Tris–HCl (pH 7.5), 150 mM NaCl, 5 mM EDTA (pH 8.0), 0.1% Triton X-100 and 0.2% NP-40, with freshly added 10 mM PMSF, 20 mM MG132 and a protease inhibitor cocktail (Roche). Approximately 5 μg OsPIL15-His protein was mixed with the total protein extracts from WT or *PHYB-GFP* plants and then incubated overnight with anti-GFP (MBL, Nagoya, Japan) conjugated beads at 4°C under red-light conditions. The beads were then washed five times with 2-ml lysis buffer and eluted samples were analyzed by immunoblotting with anti-GFP (1 : 2000; Roche Diagnostics) and anti-His (1 : 3000; CWBIO, Beijing, China) antibodies.

Results

OsmiR530 regulates grain yield by altering grain size and panicle architecture

In order to investigate the functions of OsmiR530 related to rice growth and development, we generated miR530-OE and MIM530 lines. The expression of OsmiR530 and the target mimic were under the control of a constitutively active ubiquitin promoter. The qRT-PCR analyses indicated that the expression levels of OsmiR530 in the miR530-OE lines and the OsmiR530 target mimic in the MIM530 lines were significantly elevated to varying degrees (Fig. S1a,b). The miR530-OE plants exhibited dwarfism (*c.* 78.3% of the WT height; $P < 0.01$) (Figs 1a, S1c). Compared with the WT plants, the miR530-OE plants produced shorter panicles (*c.* 77.8% of the WT panicle length; $P < 0.01$) and more aborted seeds (*c.* 64.4% of the WT seed-setting rate; $P < 0.01$) (Figs 1b, S1d–f). Further analyses of the panicle indicated that compared with the WT plants, the miR530-OE lines had considerably fewer primary (*c.* 93.8% of WT; $P < 0.05$) and secondary (*c.* 68.0% of WT; $P < 0.001$) branches and fewer effective grains per main panicle (*c.* 66.1% of WT; $P < 0.001$) (Fig. 1c). Moreover, the grain length and width and 1000-grain weight decreased significantly in the miR530-OE lines (Fig. 1d–f). In contrast to the miR530-OE plants, the MIM530 plants were taller than the WT plants and produced longer panicles, more panicle branches and larger seeds (Figs 1a–f, S1c–g). The grain length, grain width and 1000-grain weight also were significantly greater for the MIM530 lines than for the WT plants (Fig. 1d–f).

The number of vascular bundles in the peduncle is reportedly related to the number of panicle branches and grains (Ikeda-Kawakatsu *et al.*, 2009; Terao *et al.*, 2010). Correspondingly, compared with the peduncle diameter of the WT plants, those of the miR530-OE and MIM530 lines were smaller and larger, respectively (Fig. S2a). Transverse sections of the internode just below the neck node revealed that there were considerably fewer large and small vascular bundles in the miR530-OE lines than in the WT plants, whereas there were more vascular bundles in the MIM530 lines (Fig. S2b–d). These results suggest that OsmiR530 affects the formation of vascular bundles in the peduncle, which influences the peduncle diameter and panicle branching.

The grain yields of the WT plants and the miR530-OE and MIM530 lines were determined in field plots in Jinan, China (lat 36°40′N, long 117°00′E) to evaluate the effect of OsmiR530. Compared with the grain yield of WT plants, those of the miR530-OE and MIM530 lines were *c.* 43.29% lower and *c.* 7.93% higher, respectively (Table 1). Overall, these results indicate that OsmiR530 negatively regulates rice yield.

Spatial and temporal expression pattern of OsmiR530

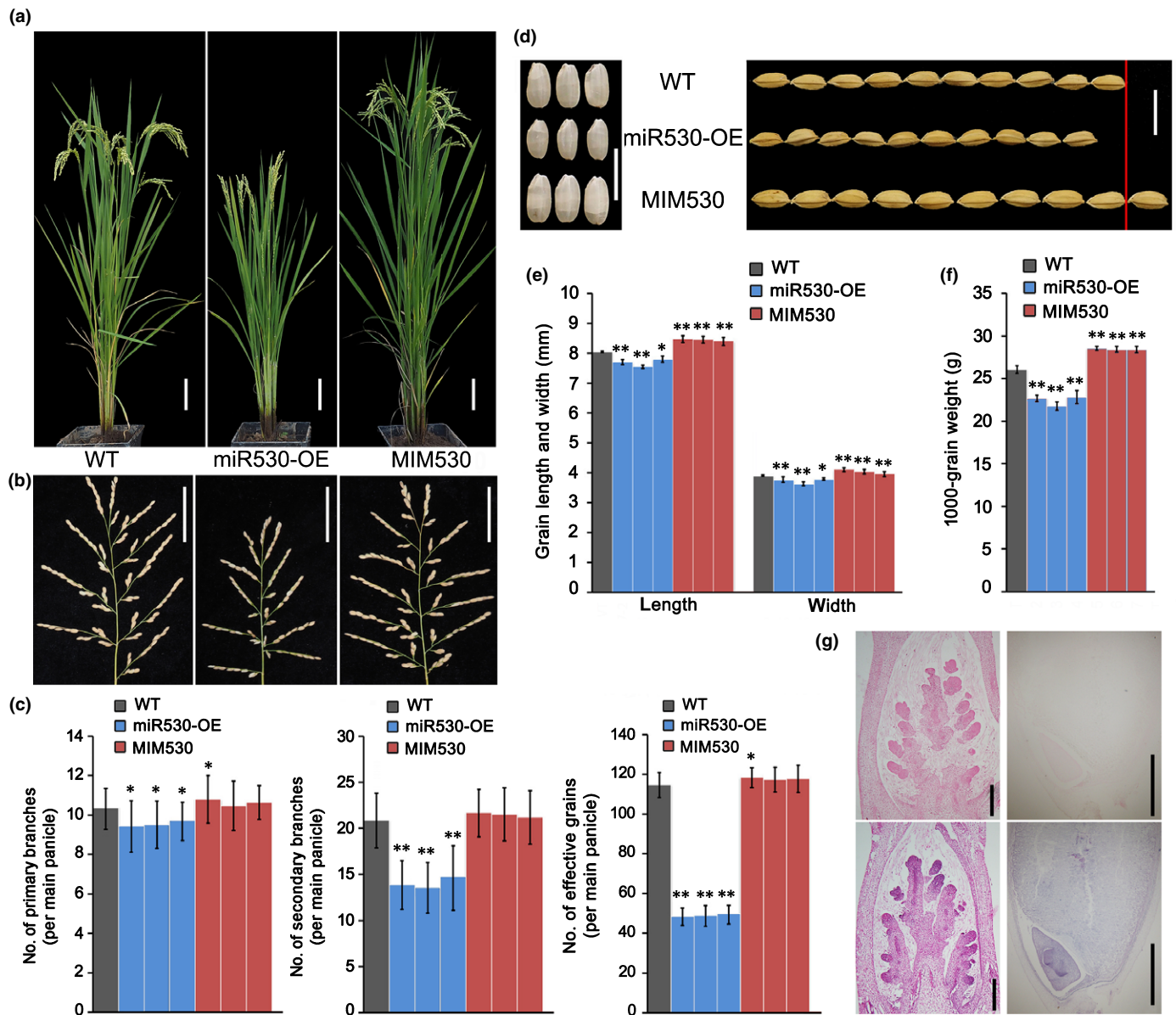MicroRNA expression patterns may provide clues regarding its functions. Thus, OsmiR530 expression was examined in

Fig. 1 Phenotypes and agronomic traits of OsmiR530-overexpressing (miR530-OE) and target mimic (MIM530) lines (miRNA, microRNA; Os, *Oryza sativa*). (a) Morphologies of rice transgenic and wild-type (WT) plants. Bars, 10 cm. (b) Panicle morphologies of the rice transgenic and WT plants. Bars, 5 cm. (c) Number of primary and secondary branches and number of effective grains per main panicle in rice transgenic and WT plants. (d) Brown rice grains (left) and grains with hulls (right) of rice transgenic and WT plants. Bars, 1 cm. (e) Grain length and width of rice transgenic and WT plants. (f) The 1000-grain weight of rice transgenic and WT plants. (g) *In situ* hybridization of OsmiR530 in the panicle at the secondary branch formation stage (left column) and in the seed at 8 d after pollination (right column) in rice. The upper panels are the negative controls. Bars, 200 μm (left column), and 1 mm (right column). For all histograms, gray bars represent WT, blue bars represent miR530-OE transgenic lines #a1, #b5 and #c2 (from left to right), and red bars represent MIM530 transgenic lines #2, #3 and #6 (from left to right). The data in (c), (e) and (f) are presented as the mean ± SD (c, $n = 20$ plants; e, $n > 300$ seeds; f, $n = 3$ replicates). Significant differences: *, $P < 0.05$; **, $P < 0.01$ (Student's t-test).

the root, flag leaf, node, panicle, embryo and seed. The qRT-PCR data indicated that OsmiR530 was expressed in all examined organs, especially in the flag leaf (Fig. S3a). Previous studies on rice revealed that the photosynthetic products related to grain-filling are derived mainly from the top three leaves, especially the flag leaf (Al-Sady *et al.*, 2006; Yue *et al.*, 2006). Therefore, the accumulation of OsmiR530 in the flag leaf implies that it may have an important effect on grain yield. Consistent with this possibility, overexpression or repressed expression of OsmiR530 altered the panicle architecture and grain size (Fig. 1). We performed an RNA *in situ* hybridization experiment to examine OsmiR530 expression in the inflorescence meristem and seeds at 8 d after pollination. OsmiR530 was strongly expressed in the secondary branch primordia (Fig. 1g, left column) at the late secondary branch formation stage. In seeds, intense and weak OsmiR530 signals were detected in the embryo and endosperm cells, respectively (Fig. 1g, right column).

Table 1 Rice grain yields of wild-type (WT), OsmiR530-overexpressing (miR530-OE) and OsmiR530 target mimic (MIM530) rice lines, and knockout PLUS3-domain-containing protein (*PL3*-KO) plants grown in a paddy field.

Traits	WT	miR530-OE	MIM530	PL3-KO
Yield per plot (kg)	1.64 ± 0.06	0.93 ± 0.09 ($P < 0.001$)	1.77 ± 0.08 ($P = 0.018$)	1.31 ± 0.07 ($P < 0.001$)
Yield comparison with WT (%)	—	−43.29	+7.93	−20.12

Plants were arranged in plots according to a randomized complete block design with four replicates. Three transgenic lines were mixed and grown in one plot. Nipponbare (WT) was used as a control. Plants were grown under natural conditions in Jinan, China in 2018. The planting density was 20 cm × 25 cm, with one plant per hill. Data are presented as the mean ± SD ($n = 4$ plots, 3.0 m^2 per plot). Significant differences were determined with Student's *t*-test.

OsmiR530 regulates grain size by controlling cell division and expansion

Because the spikelet hull restricts grain size, we measured the spikelet hulls of the WT, miR530-OE and MIM530 plants. The spikelet hulls of the miR530-OE lines were significantly shorter and thinner than those of the WT plants, whereas spikelet hulls of the MIM530 lines were longer and wider than those of the WT plants (Figs 2a, S1g). The enlargement of plant organ is generally due to cell division and expansion. To clarify the grain size changes in the transgenic lines, histological cross-sections of the spikelet hulls just before anthesis were analyzed. Compared with the WT plants, the MIM530 and miR530-OE lines had more and fewer outer parenchyma cells in the grain hull, respectively (Fig. 2b,c). These findings suggest that miR530 negatively regulates cell division in rice. Furthermore, the inner epidermal cells of the lemma in the miR530-OE, MIM530 and WT plants were analyzed by SEM. The areas of the inner epidermal cells of the spikelet followed the same rank order as the number of parenchyma cells: miR530-OE < WT < MIM530 (Fig. 2d,e). The increasing epidermal cell areas in the MIM530 lines were due mainly to increases in cell length, but not cell width (Fig. 2f, g). These results imply that repressing the expression of OsmiR530 sufficiently promotes the cell expansion and proliferation in the spikelet hulls to produce larger seeds.

OsPL3 is a direct target of OsmiR530

In plants, miRNAs exert their functions by inhibiting the expression of their target genes. To uncover the molecular mechanism underlying the regulatory function of OsmiR530 influencing rice yield, we identified its downstream targets by two methods. A previous study predicted that one of the genes targeted by OsmiR530 is *OsPL3* (LOC_Os01g56780), which encodes a PLUS3 domain-containing protein. *OsPL3* mRNAs were spliced between the 10th and 11th base pair of the OsmiR530 target region based on degradome sequencing result (Sun *et al.*, 2015). To further validate the target, we performed RLM5′-RACE to map the OsmiR530-directed cleavage sites in *OsPL3* mRNA. Of 15 randomly selected clones, 13 possessed the 5′ ends of the cleaved fragments at the same site of the OsmiR530 target sequence as that detected by degradome sequencing (Fig. 3a), indicating that *OsPL3* can be precisely cleaved by OsmiR530 *in vivo*.

We then investigated the spatial expression patterns of *OsPL3* in various rice organs using qRT-PCR. Similar to OsmiR530,

OsPL3 was detected in most of the tissues analyzed, especially in the flag leaf (Fig. S3b). The results of an RNA *in situ* hybridization revealed that *OsPL3* also was expressed in the primordia of the secondary panicle branches in the inflorescence meristem (Fig. 3b). Strikingly, the *OsPL3* expression patterns were anti-correlated with OsmiR530 in the examined floral organs and seeds (Fig. S3). Additionally, *OsPL3* expression was significantly downregulated in the miR530-OE lines and upregulated in the MIM530 lines (Fig. 3c), suggesting that OsmiR530 negatively regulates *OsPL3* expression. These results imply that the *OsPL3* expression level is dependent on the level of OsmiR530 through an OsmiR530-directed cleavage mode *in vivo*.

In order to elucidate the function of *OsPL3* related to rice panicle and seed development, we generated three independent *OsPL3*-knockout (*PL3*-KO) lines in the Nip background using CRISPR/Cas9 technology. The *PL3*-KO1 (#12) plants had a 10-bp deletion in the third exon of *OsPL3*, whereas the *PL3*-KO2 (#13) and *PL3*-KO3 (#16) plants had a single base (A) inserted in the third exon at 1693 and 1797 bp from the translation start site, respectively (Fig. S4). The deletion or insertions created new stop codons that result in a truncated OsPL3 lacking the PLUS3 domain (Fig. S5). As expected, the three *PL3*-KO lines showed similar phenotypes as those of miR530-OE plants, including dwarfism, smaller panicles, decreased effective grains per main panicle, low seed-setting rate, fewer secondary branches per main panicle and smaller seeds (Figs 3d–j, S6). A field trial showed that knocking out *OsPL3* led to *c.* 20.12% yield losses (Table 1). These results confirmed that *OsPL3* is the major target of OsmiR530 related to the regulation of panicle and seed development in rice.

Protein structure analysis revealed that OsPL3 contains a PLUS3 domain in the C-terminal, which is essential for nucleic acid binding. Subcellular localization in rice protoplasts detected OsPL3 in the nucleus (Fig. 3k). However, the molecular mechanism by which OsPL3 affects panicle branching and seed development in rice remains to be characterized.

OsPIL15 directly activates *OsMIR530* transcription to regulate grain size and panicle architecture

In order to identify the upstream regulators of OsmiR530, the 2-kb upstream sequence of *OsMIR530* promoter was analyzed, and three G-box elements were identified. Because the G-box is the core element for the targets of PIFs and PILs (Martínez-García *et al.*, 2000; Castillon *et al.*, 2007; Hornitschek *et al.*, 2009;
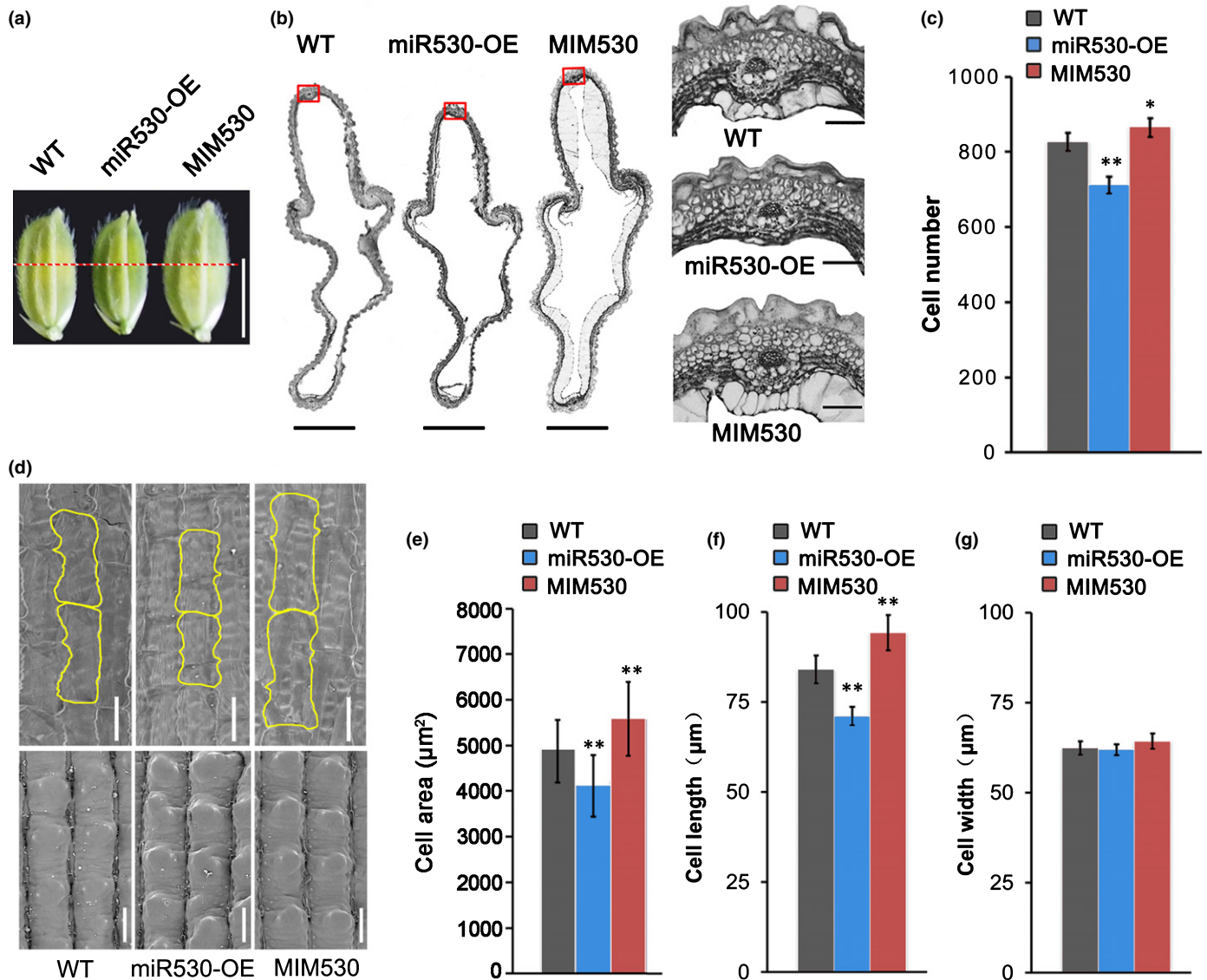
Fig. 2 Histological analysis of spikelet hulls in OsmiR530 transgenic lines and wild-type (WT) plants (miRNA, microRNA; Os, *Oryza sativa*). (a) Spikelet hulls of rice WT and transgenic plants just before anthesis. Bar, 5 mm. (b) Cross-sections of the middle parts of spikelet hulls (marked by red dashed lines in a) of rice WT and transgenic plants just before anthesis (left). Bars, 500 μm. Magnified images of the boxed cross-section areas are provided on the right. Bars, 50 μm. (c) Number of cells in the outer parenchyma layer of the spikelet hulls of rice WT and transgenic plants (*n* = 5 spikelets). (d) Scanning electron micrographs of the inner epidermal cells of lemmas in the mature seeds of rice WT and transgenic plants. Bars, 50 μm. (e) Cell areas in the middle part of the inner epidermis of lemmas in fully mature rice seeds (*n* = 5 seeds). (f) Cell lengths in the middle part of the inner epidermis of lemmas in fully mature rice seeds (*n* = 5 seeds). (g) Cell widths in the middle part of the inner epidermis of lemmas in fully mature rice seeds (*n* = 5 seeds). The data in (c), (e), (f) and (g) are presented as the mean ± SD. Significant differences: *, $P < 0.05$; **, $P < 0.01$ (Student's *t*-test).

Leivar & Quail, 2011), we assumed that the rice PIL family members might be able to bind to the *OsMIR530* promoter.

Among the six *PIL* genes (*OsPIL11–16*) in the rice genome (Nakamura *et al.*, 2007), *OsPIL15* was identified to play important roles in grain size regulation (Ji *et al.*, 2019). We also analyzed the *PIL15*-OE (Zhou *et al.*, 2014) and *PIL15*-KO transgenic lines (Figs 4, S7, S8). Consistent with the results of a recent study (Ji *et al.*, 2019), the *PIL15*-OE lines produced smaller seeds than the WT plants, whereas the *PIL15*-KO lines produced larger seeds (Fig. 4a–c). Additionally, we observed that *OsPIL15* negatively regulates secondary branching. The *OsPIL15*-OE plants had significantly fewer secondary branches

compared with the WT plants, whereas the *OsPIL15*-KO plants had considerably more secondary branches (Fig. 4d). The phenotypic similarities between the *OsPIL15*-OE and miR530-OE plants, and between the OsPIL15-KO and MIM530 plants suggest that OsPIL15 may directly regulate *OsMIR530* expression.

The three G-box elements identified in the *OsMIR530* promoter were located < 600 bp from the *OsMIR530* transcription start site and were divided artificially into fragments A and B (Fig. 5a). The interaction between OsPIL15 and the *OsMIR530* promoter was first assessed in a Y1H assay, which revealed that OsPIL15 can bind to both fragments A and B with normal G-box elements (Fig. 5b). However, mutations to the G-box
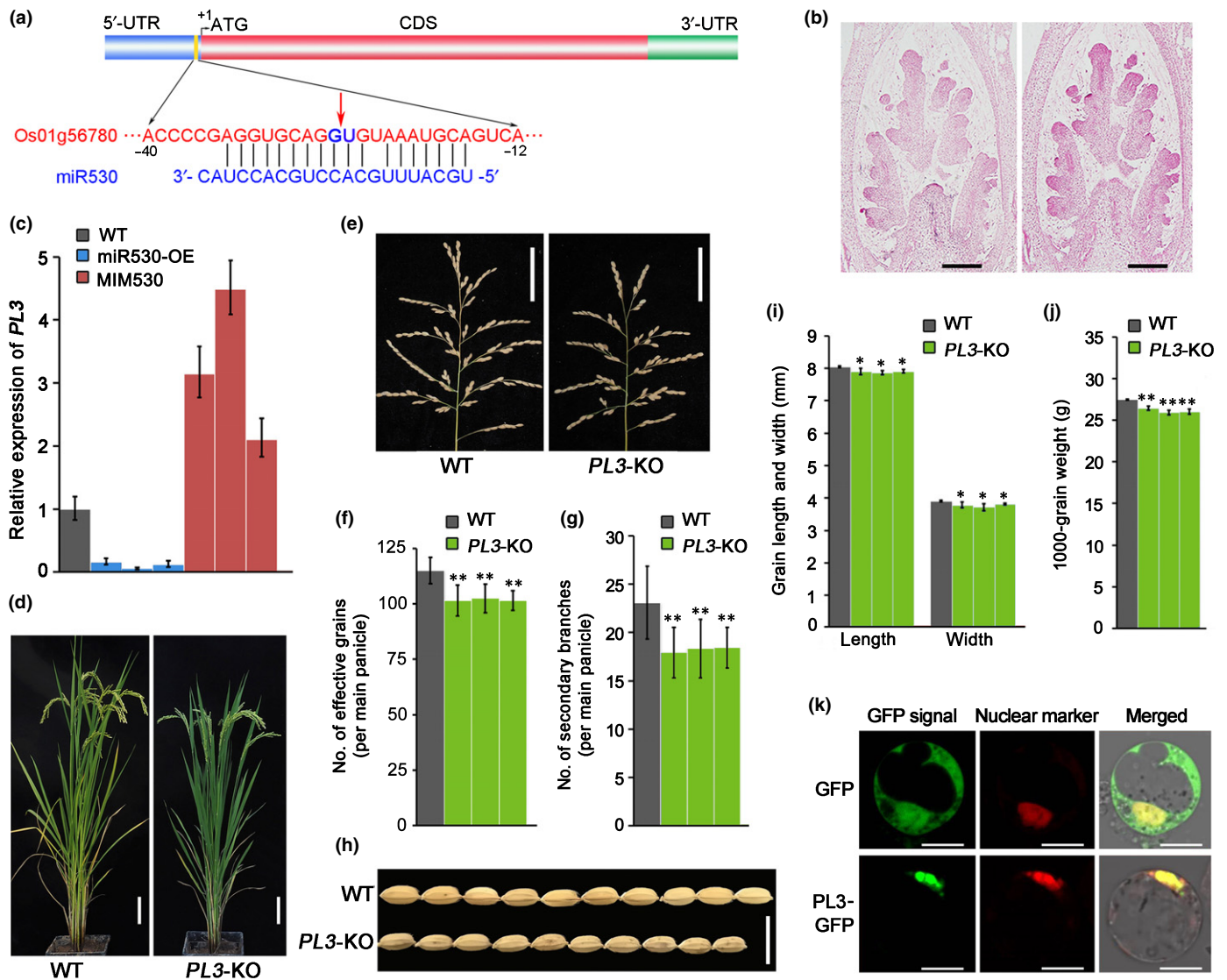
Fig. 3 Phenotypes and agronomic traits of *OsPL3*-knockout (PL3-KO) lines (Os, *Oryza sativa*; PL3, PLUS3-domain-containing protein). (a) Illustration of the OsmiR530 cleavage site in the *OsPL3* mRNA. (b) *In situ* hybridization of *OsPL3* in the panicle at the secondary branch formation stage in rice. The left graph presents the data for the negative control (sense probe). Bars, 200 μm. (c) The expression of *OsPL3* in OsmiR530-overexpressing (miR530-OE) and OsmiR530 target mimic (MIM530) rice lines. The *OsEF-1α* gene was used as an internal reference for quantitative real-time (qRT)-PCR. Data are presented as the means ± SD of three biological replicates. (d) Morphologies of rice *PL3*-KO and wild-type (WT) plants. Bars, 10 cm. (e) Panicle morphologies of the rice *PL3*-KO and WT plants. Bars, 5 cm. (f) Number of effective grains per main panicle in rice *PL3*-KO and WT plants. (g) Number of secondary branches in rice *PL3*-KO and WT plants. (h) Grains with hulls from rice WT and *PL3*-KO plants. Bar, 1 cm. (i) Grain length and width of rice transgenic and WT plants. (j) The 1000-grain weight of rice transgenic and WT plants. (k) Subcellular localization of OsPL3 in rice protoplasts. Bars, 10 μm. For all histograms, gray bars represent WT, green bars represent *PL3*-KO transgenic lines #12, #13 and #16 (from left to right). The data in (c), (f), (g), (i) and (j) are presented as the mean ± SD (f and g, *n* = 20 plants; i, *n* > 300 seeds; j, *n* = 3 replicates). Significant differences: *, *P* < 0.05; **, *P* < 0.01 (Student's *t*-test).

elements of these two fragments in the *OsMIR530* promoter abolished this binding (Fig. 5b). To further determine whether the G-box element in the *OsMIR530* promoter is the direct binding site for OsPIL15, we conducted EMSA with the purified OsPIL15-His recombinant protein and *OsMIR530* probes with normal and mutated G-box elements. As presented in Fig. 5(c), OsPIL15 specifically bound to *OsMIR530* promoter fragments A and B with the normal G-box sequence. The binding abilities to the two fragments decreased significantly in the presence of unlabeled competitor probes A and B, but not with the unlabeled

probes with mutated G-box sequences (Fig. 5c). These results suggest the G-box motif is critical for the binding of OsPIL15 to the *OsMIR530* promoter. A ChIP-qPCR analysis was performed with the *OsPIL15-eGFP* lines, which have phenotypes similar to those of *PIL15*-OE lines (Fig. 4). The enrichment of fragments A and B containing one or two G-box motifs in the 2-kb sequence upstream of the *OsMIR530* promoter was analyzed, with a fragment C located 1950 bp upstream of the *OsMIR530* transcription start site used as a negative control (Fig. 5a). As shown in Fig. 5(d), fragments A and B were obviously enriched in the
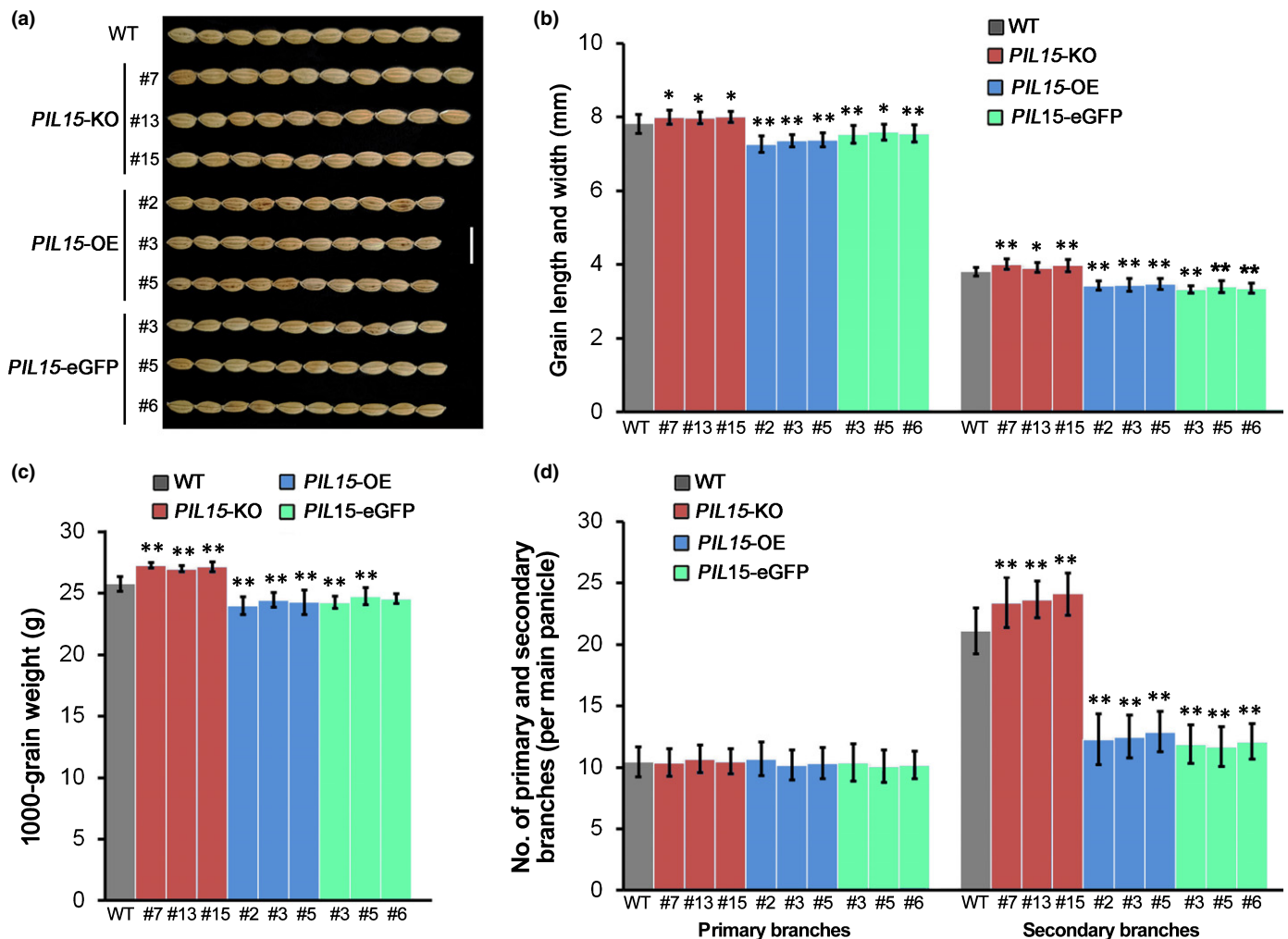
Fig. 4 Agronomic traits of *OsPIL15*-overexpressing (*PIL15*-OE and *PIL15*-eGFP) and knockout (*PIL15*-KO) transgenic lines (GFP, green fluorescent protein; Os, *Oryza sativa*: PIL, phytochrome-interacting factor (PIF)-like gene). (a) Grains with hulls (right) from rice wild-type (WT) and transgenic plants. Bar, 1 cm. (b) Grain length and width of rice WT and transgenic plants. (c) The 1000-grain weight of rice WT and transgenic lines. (d) Number of primary and secondary branches in rice WT and *OsPIL15* transgenic plants. The data in (b), (c) and (d) are presented as the mean ± SD (b, $n > 300$ seeds; c, $n = 3$ replicates; d, $n = 20$ panicles). Significant differences: *, $P < 0.05$; **, $P < 0.01$ (Student's t-test).

PIL15-eGFP plants, whereas fragment C was not. These results further indicate that OsPIL15 binds to the G-box elements in the *OsMIR530* promoter region.

In order to determine how OsPIL15 regulates *OsMIR530* expression, we detected the expression of the OsmiR530 precursor (*OsMIR530*) and the mature OsmiR530 in *PIL15*-OE and *PIL15*-KO lines. The *OsMIR530* transcripts obviously accumulated in the *PIL15*-OE lines, but decreased in *PIL15*-KO lines (Fig. 5e). The mature OsmiR530 and its precursor *OsMIR530* exhibited similar expression patterns in *OsPIL15* transgenic lines (Fig. S9). These results imply that the expression of *OsMIR530* is positively correlated with that of *OsPIL15*. We subsequently conducted transient expression assays to confirm the *in vivo* result. The *A. tumefaciens* strains harboring the p35S:OsPIL15 effector and pOsMIR530:LUC reporter plasmids were used to infiltrate *N. benthamiana* leaf epidermal cells. The LUC activity was examined after a 2-d incubation in darkness. The co-expression of p35S:OsPIL15 and pOsMIR530:LUC sharply increased the

LUC reporter activity, in contrast to the effects of the empty vector control (Fig. 5f). Overall, these results demonstrate that OsPIL15 can activate *OsMIR530* expression *in vivo* by directly binding to the promoter G-box elements.

Evolution and genetic variations in OsmiR530

By screening the miR530 family in the miRBase database, we determined that miR530 is specific to plants. Most plant species, including rice, have only one miR530 member in their genomes, but the *Glycine max* genome has the most miR530 family members (Gma-miR530a, b, c, d and e) (Fig. S10). Compared with the mature osa-miR530-5p sequence in miRBase, the OsmiR530 identified in the *phyB* mutant and WT (Nip) plants contains an additional base (cytosine) at the 3′ end. Both osa-miR530-5p and OsmiR530 were derived from the same precursor and osa-miR530-5p was not detected in the *phyB* mutant and Nip small RNA libraries. These observations suggest that OsmiR530 is the
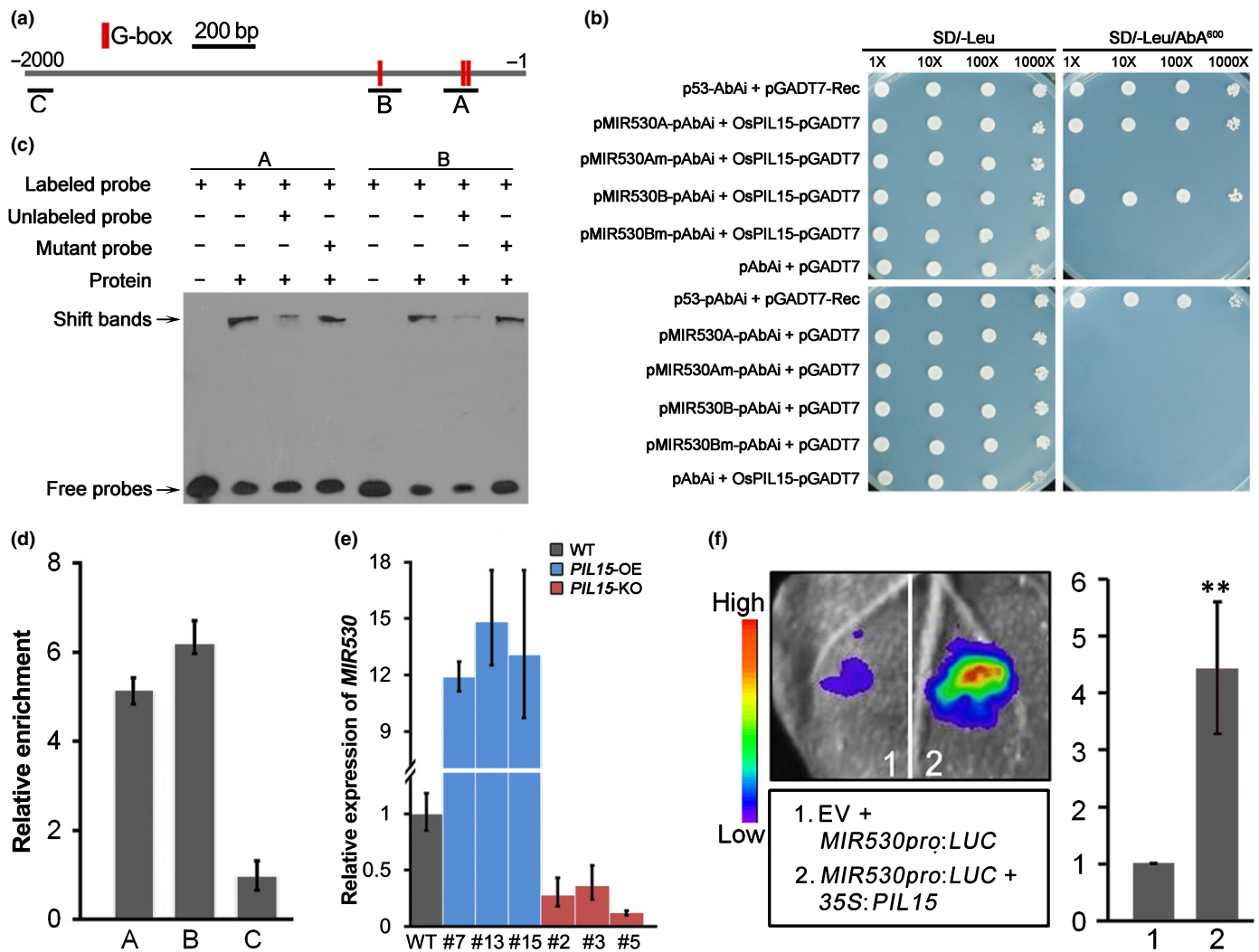
Fig. 5 Identification of the *OsMIR530* gene as a direct target of OsPIL15 (miRNA, microRNA; Os, *Oryza sativa*; PIL, phytochrome-interacting factor (PIF)-like gene). (a) Schematic representation of G-box elements in the *OsMIR530* promoter. (b) Yeast-one-hybrid assay of the binding of OsPIL15 to the *OsMIR530* promoter. Two fragments containing two adjacent G-box and one single G-box elements were synthesized, and then were separately inserted into the reporter vector pAbAi to obtain the pMIR530A-AbAi and pMIR530B-AbAi construct, respectively. Meanwhile, the pMIR530Am-AbAi and pMIR530Bm-AbAi constructs were obtained using the same sequences with mutated G-box elements. pGADT7-Rec-p53 and p53-AbAi were used as positive controls. (c) Electrophoretic mobility shift assay. Unlabeled probes containing G-box elements at 50× the amount of the labeled probe competed for the *OsPIL15* binding sites. Unlabeled probes with mutations in G-box elements were also used in this assay. (d) Chromatin immunoprecipitation and quantitative real-time (qRT)-PCR analysis of OsPIL15 binding to the *OsMIR530* promoter. The DNA samples acquired before immunoprecipitation were used as the input, and IgG was set as a negative control. The qRT-PCR was completed with three replicates. Signal intensities were first normalized relative to the input, then the enrichment of each fragment was calculated using the Input% of IgG as a baseline. (e) Expression of *OsMIR530* (OsmiR530 precursor) in rice *PIL15*-OE and *PIL15*-KO transgenic plants. The *OsEF-1α* gene was used as an internal reference for the qRT-PCR. Data are presented as the mean ± SD of three biological replicates. (f) Transient expression assays indicated that *OsMIR530* transcription was activated by OsPIL15. Representative images of *Nicotiana benthamiana* at 48 h post-infiltration (left). More than 10 independent *N. benthamiana* leaves were infiltrated in the experiment. The histogram (right) presents the intensities of the luminescence indicated in the photo (left). Significant differences: *, $P < 0.05$; **, $P < 0.01$ (Student's *t*-test).

main miR530 family member in our plant materials. Additionally, OsmiR530 homologs were not identified in the genomes of the widely used model plants *Arabidopsis* and maize. These findings imply that miR530 has unique functions during plant divergence and speciation.

Considering that OsmiR530 plays an important role in mediating rice grain yield, we explored the variations in the mature miR530 sequence as well as in its precursor sequence and its

promoter sequences among 3024 rice varieties in the 3000 Rice Genome Project (Zheng *et al.*, 2015). No polymorphisms were identified in the mature sequences of all rice varieties, whereas three single nucleotide polymorphisms (SNPs), G/A-C/T-G/A, were identified in the miR530 precursor sequences (Fig. 6a). Most of the rice varieties (97.7%, 2953 of 3024) were classified into two haplotypes (HAP1 with G-C-G SNPs and HAP2 with A-T-A SNPs in the miR530 precursor sequences, respectively)

(Fig. 6a,b). The majority of *indica* varieties (98.6%, 1733 of 1758) were HAP1 haplotype (Fig. 6b). By contrast, the occurrence of the HAP2 haplotype was observed mainly in the *temperate japonica* (92.3%, 250 of 271) and *subtropical japonica* (75.9%, 85 of 112) varieties (Fig. 6b). However, the functional significance of these three SNPs remains elusive. In the *OsMIR530* promoter regions, 13 SNPs and three insertion–deletion polymorphisms (InDels) were identified in all examined rice accessions (Fig. 6a). Given that InDels cause more dramatic alterations to the genome structure than SNPs, subsequent analyses were focused on the InDels in the *OsMIR530* promoter regions (Fig. 6c). Most of the rice accessions (99.1%, 2998 of 3024) were classified into three haplotypes (*MIR530^{NIP}*, *MIR530^{MH63}* and *MIR530^{GL4}*) represented by Nip, Minghui63 (MH63) and Guangluai4 (GL4), respectively. The *MIR530^{NIP}* and *MIR530^{MH63}* haplotypes have a single 6-bp (5′-AGATGG-3′) and 4-bp (5′-CATA-3′) insertion at different positions, respectively (Fig. 6a). The *MIR530^{GL4}* haplotype has both insertions in the promoter region (Fig. 6a). The majority of *japonica* varieties were the *MIR530^{NIP}* haplotype, as indicated by the 93.4% (268 of 287), 76.1% (86 of 113) and 58.5% (48 of 82) occurrence in the *temperate japonica*, *subtropical japonica* and *admixed japonica* varieties, respectively (Fig. 6c). Only a small portion of the *tropical japonica* varieties (12.6%, 47 of 372) were classified as the *MIR530^{NIP}* haplotype. Additionally, occurrences of *MIR530^{MH63}* haplotype in *centrum-Aus* and *indica* varieties were 41.4% (82 of 198) and 34.5% (611 of 1771), respectively. However, the greater frequency of the *MIR530^{GL4}* haplotype was observed not only in the *centrum-Aus* (54.0%, 107 of 198) and *indica* (61.0%, 1080 of 1771) varieties, but also in the *tropical japonica* varieties (86.3%, 321 of 372). Interestingly, HAP1 based on three SNPs in the miR530 precursor sequences was well correlated with *MIR530^{MH63}* and *MIR530^{GL4}*, whereas HAP2 was correlated with *MIR530^{NIP}* (Fig. 6d). These results suggest that the *OsMIR530* locus was subjected to artificial selection during rice breeding.

Discussion

Grain size and panicle branching, which are controlled by complex genetic networks, are two key factors influencing grain yield. Although a number of genes regulating grain yield have been identified, considerably fewer microRNAs (miRNAs) have been confirmed as important regulators of grain yield.

In this study, OsmiR530 was confirmed as a negative regulator of rice grain yield via affecting cell division and expansion in spikelet hulls. The overexpression of OsmiR530 decreased the seed size and inhibited panicle branching, whereas the OsmiR530 target mimic had the opposite effects (Fig. 1). To the best of our knowledge, this is the first report describing miR530 as a potential regulator of grain yield. Four other miRNAs have been confirmed as important regulators of rice grain yield, namely OsmiR156 (Jiao *et al.*, 2010; Wang *et al.*, 2012; Si *et al.*, 2016), OsmiR396 (Duan *et al.*, 2015; Gao *et al.*, 2015), OsmiR397 (Y. C. Zhang *et al.*, 2013) and OsmiR408 (Zhang *et al.*, 2017). Although the effects of the previously reported miRNAs on grain yield are clear, their upstream factors were uncharacterized. In this study, we determine that OsmiR530 expression can be activated by phytochrome-interacting factor (PIF)-like gene OsPIL15 (Fig. 5), which is one of the homologs of *Arabidopsis* PIFs. Knocking out *OsPIL15* enhances cell division in spikelet hulls, resulting in enlarged rice grains (i.e. longer and wider) and increased grain yield (Ji *et al.*, 2019). Moreover, in this study, we observed that similar to OsmiR530, OsPIL15 negatively regulates grain yield by controlling grain size as well as panicle branching. The *PIL15*-OE lines produced smaller seeds and fewer panicle branches compared with the wild-type (WT) plants, whereas the knockout (*PIL15*-KO) lines exhibited the opposite phenotypes (Fig. 4). These results suggest that OsPIL15 has important regulatory roles influencing grain size and panicle branching.

PIFs are believed to be one of the major targets of photoactivated phytochromes in *Arabidopsis* (Nakamura *et al.*, 2007; Leivar & Quail, 2011). In the present study, we observed that *OsMIR530* expression can be activated by OsPIL15 (Fig. 5). Additionally, the OsmiR530 expression is significantly upregulated in the *phytochrome B* (*phyB*) mutant (Sun *et al.*, 2015). Thus, clarifying the relationship between OsPIL15 and PHYB is warranted. Accordingly, in the current study, we proved that OsPIL15 interacts physically with PHYB *in vitro* and *in vivo* (Fig. S11), which is consistent with the result from a recent study involving a bimolecular fluorescence complementation system (Xie *et al.*, 2019). However, it was unclear how OsPIL15 and PHYB coordinately control rice grain size. Xie *et al.* (2019) revealed that the light-induced degradation of OsPIL15 is partially dependent on PHYB in rice. In this context, there should be more OsPIL15 in the *phyB* mutant than in the WT control. We observed that the *phyB* mutant had smaller seeds (Fig. S12), resembling those of *OsPIL15*-OE (Fig. 4). Thus, the direct interaction between PHYB and OsPIL15 regulates grain size by inducing the degradation of OsPIL15 and decreasing OsmiR530 expression.

The degradation of PIFs or PILs is essential for activating or repressing the expression of their downstream genes (Nakamura *et al.*, 2007; Leivar & Quail, 2011). A recent study indicated that OsPIL15 upregulates the expression of a purine permease gene, *OsPUP7*, by binding to the N-box (5′-CACGCG-3′) motifs in the promoter (Ji *et al.*, 2019). The rice grains of the loss-of-function mutant *ospup7*, are significantly larger than those of the control (Zhonghua 11) (Qi & Xiong, 2013), which is consistent with the effects of a loss-of-function mutation to *OsPIL15* (Ji *et al.*, 2019). Although the 50-seed weight of the *ospup7* mutant is *c.* 125% greater than that of Zhonghua 11, the mutant produces *c.* 50% fewer tillers and spikelets per panicle than the control (Qi & Xiong, 2013). Thus, it is obvious that the reported increased grain yield of *OsPIL15*-knockout plants (Ji *et al.*, 2019) is not due to OsPUP7. In the present study, we identified *OsMIR530* as a critical target of OsPIL15. Moreover, OsPIL15 can bind directly to the G-box in the *OsMIR530* promoter region to activate its expression (Fig. 5b–f). Most importantly, the phenotypes of the *PIL15*-KO and *PIL15*-OE lines were highly similar to those of the MIM530 and miR530-OE lines, respectively (Fig. 4). Thus, we conclude that OsPIL15 regulates grain yield mainly by controlling OsmiR530 expression.
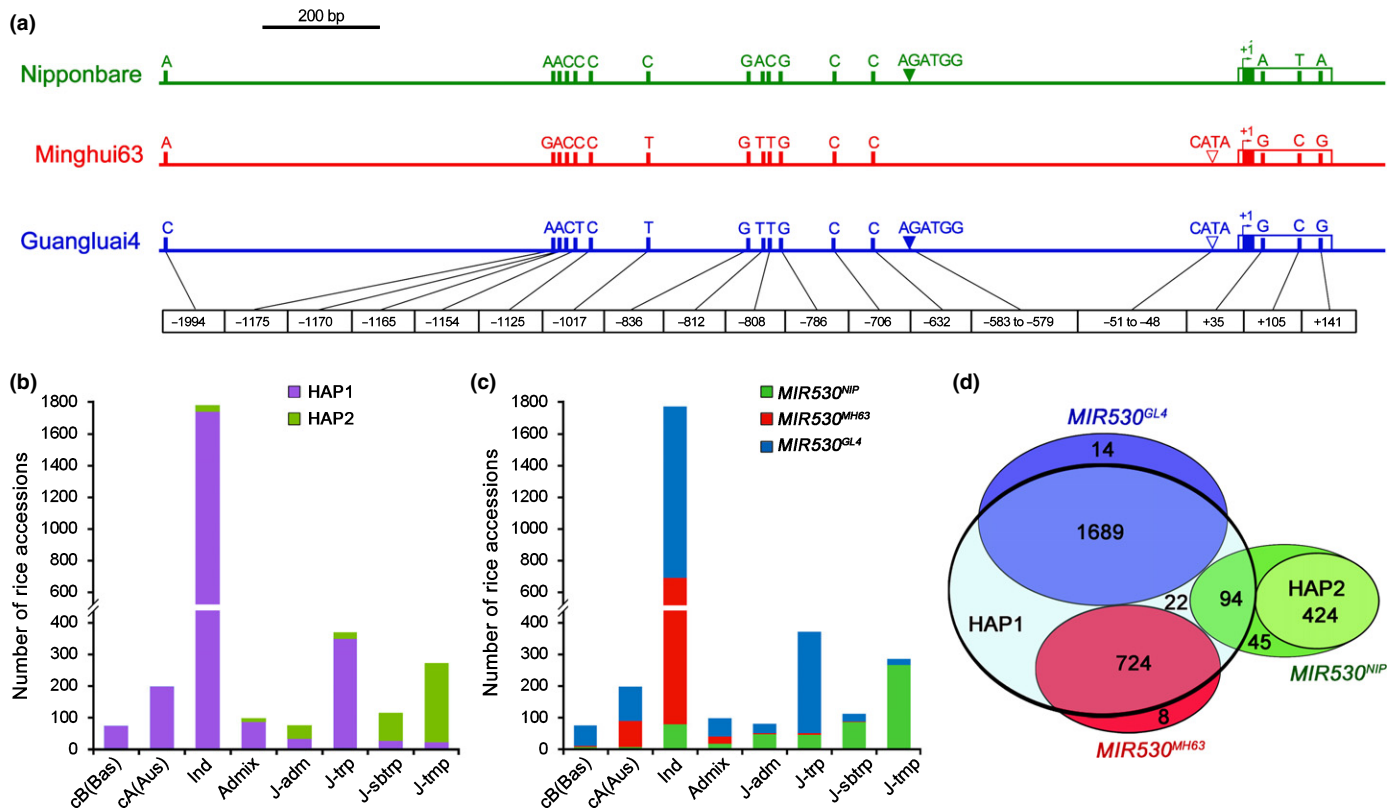
Fig. 6 Analysis of genetic variations in *OsMIR530* (miRNA, microRNA; Os, *Oryza sativa*). (a) Schematic representation of the genetic variations in *OsMIR530* in a *japonica* variety (Nipponbare) and two *indica* varieties (Minghui63 and Guangluai4). The white boxes at the 3′ terminal represent the pre-OsmiR530, which contains the mature OsmiR530 sequences of indicated by solid boxes marked in green, red and blue, respectively. The promoter sequence is presented with lines. The numbers at the bottom indicate the positions of the variations (The 5′ terminal nucleotide of the mature OsmiR530 is referred to as +1). (b) Distribution of three single nucleotide polymorphisms (SNPs) in the miR530 precursor sequences in 2953 rice varieties. The classification of the rice varieties is based on the 3000 Rice Genome Project database. (c) Distribution of three haplotypes of insertion–deletion polymorphisms (InDels) in the *OsMIR530* promoter in 2998 rice varieties. (d) Schematic representation of the relationship between the three SNPs in the OsmiR530 precursor sequence and the three InDel polymorphisms in the *OsMIR530* promoter sequence. NIP, Nipponbare; MH63, Minghui63, GL4, Guangluai4; cB (Bas), *centrum-Basmati* population; cA(AUS), *centrum-Aus* population; Ind, *indica* rice; Admix, admixed between any two or more of *indica*, *japonica*, cA(AUS) and cB (Bas); J-adm, *admixed japonica* with two or more *japonica* subpopulations; J-trp, *tropical japonica*; J-sbtrp, *subtropical japonica*; J-tmp, *temperate japonica*.
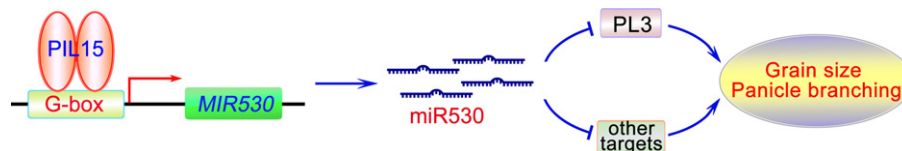
Fig. 7 Proposed working model of the regulation of rice grain yield by the OsPIL15-OsmiR530 module (miRNA, microRNA; Os, *Oryza sativa*; PIL, phytochrome-interacting factor (PIF)-like gene). The accumulation of OsPIL15 promotes *OsMIR530* transcription. The overexpression of *OsMIR530* leads to the accumulation of mature OsmiR530, which downregulates *OsPL3* expression, thereby inhibiting grain size enlargement and panicle branching.

In this study, we identified *OsPL3*, which encodes a PLUS3-domain-containing protein, is directly targeted by OsmiR530 to regulate rice branching and grain size. Knocking out *OsPL3* decreased the overall grain yield by ≤ 20.12% in a field trial (Table 1), but it cannot completely explain the 42.29% decrease in the grain yield of miR530-OE lines (Table 1). In this context, we speculate that OsmiR530 decreases the grain yield partially by downregulating *OsPL3* expression and that other targets probably also are involved in OsmiR530-regulated grain yield. The PLUS3 domain is involved in nucleotide binding, especially for RNA and single-stranded DNA (de Jong *et al.*, 2008). Previous studies

on human and yeast revealed that the PLUS3 domain affects transcriptional elongation, chromatin re-organization and co-transcriptional splicing (Ciftci-Yilmaz & Mittler, 2008; de Jong *et al.*, 2008; Wier *et al.*, 2013). The only functionally characterized PLUS3 domain containing protein in plant is AtTZP in *Arabidopsis*, wherein it is important for regulating morning-specific growth (Loudet *et al.*, 2008) and initiating the flowering process (Kaiserli *et al.*, 2015). Unlike AtTZP, which contains a zinc finger domain and a PLUS3 domain at its C-terminal, OsPL3 has only a PLUS3 domain at the C-terminal, implying that its function may differ from that of AtTZP. Thus the molecular

mechanism underlying the OsPL3-regulated rice grain yield should be explored. Considering that OsPL3 was localized to the nucleus in rice (Fig. 3k), we predict that OsPL3 is crucial for transcriptional control.

On the basis of our findings, we propose a working model for the regulatory roles of OsmiR530 in grain yield (Fig. 7). When OsPIL15 accumulates, it binds to G-box elements in the *OsMIR530* promoter to activate its expression in the nucleus. The increased production of OsmiR530 inhibits seed enlargement and panicle branching via downregulating the expression of *OsPL3* and other targets, causing substantial yield losses.

Genetic variations were identified in the *OsMIR530* promoter among 2998 rice varieties (Fig. 6). Two insertions (5′-AGATGG-3′ and 5′-CATA-3′) were detected mainly in the promoter of *indica*, *centrum-Aus* and *tropical japonica* rice, but were infrequently detected in *temperate japonica* and *subtropical japonica* rice varieties (Fig. 6a,c). However, a single insertion (5′-AGATGG-3′) in the *OsMIR530* promoter was observed mainly in *temperate japonica* and *subtropical japonica*, but rarely in *indica* and *centrum-Aus* rice (Fig. 6a,c). By contrast, another single insertion 5′-CATA-3′ in the *OsMIR530* promoter was identified relatively frequently in *indica* and *centrum-Aus* (Fig. 6a,c). It seems that two InDels were selected in the *indica* and *japonica* varieties under certain circumstances. These results imply that the *OsMIR530* locus has been artificially selected during breeding, although the functional significance of the genetic variation in *OsMIR530* remains elusive at present. Additionally, two haplotypes were identified based on three single nucleotide polymorphisms (SNPs) in the miR530 precursor (Fig. 6a,b), which are well-correlated with $MIR530^{GL4}$, $MIR530^{MH63}$ and $MIR530^{NIP}$ (Fig. 6d). Whether and how these three SNPs affect *OsMIR530* functions is one question that remains open. Moreover, the relationship between the genetic variation at the *OsMIR530* locus and the functions of the encoded miRNA, especially regarding the regulation of grain yield, is worthy of being explored comprehensively in the future.

Acknowledgements

Author contributions

XX and XHX designed the experiments, wrote and revised the paper; WS and YL performed most of the experiments with the assistance of LX, YH, XL and HS; and WL and XHX completed the bioinformatics analysis. WS and XHX contributed equally to this work.

ORCID

Yanan He https://orcid.org/0000-0002-0756-4306
Yaping Li https://orcid.org/0000-0002-9823-8492
Wen Li https://orcid.org/0000-0002-3756-4243
Xingbo Lu https://orcid.org/0000-0003-4844-0569
Hongwei Sun https://orcid.org/0000-0003-1626-5575
Wei Sun https://orcid.org/0000-0001-5890-9450
Lixia Xie https://orcid.org/0000-0002-2702-6740
Xianzhi Xie https://orcid.org/0000-0002-3245-0554
Xiao Hui Xu https://orcid.org/0000-0002-3823-0122

References

Al-Sady B, Ni W, Kircher S, Schäfer E, Quail PH. 2006. Photoactivated phytochrome induces rapid PIF3 phosphorylation prior to proteasome-mediated degradation. *Molecular Cell* 23: 439–446.

Bartel DP. 2004. MicroRNAs: genomics, biogenesis, mechanism, and function. *Cell* 116: 281–297.

Castillon A, Shen H, Huq E. 2007. Phytochrome Interacting Factors: central players in phytochrome-mediated light signaling networks. *Trends in Plant Science* 12: 514–521.

Ciftci-Yilmaz S, Mittler R. 2008. The zinc finger network of plants. *Cellular and Molecular Life Sciences* 65: 1150–1160.

Duan P, Ni S, Wang J, Zhang B, Xu R, Wang Y, Chen H, Zhu X, Li Y. 2015. Regulation of *OsGRF4* by OsmiR396 controls grain size and yield in rice. *Nature Plants* 2: 15203.

Franco-Zorrilla JM, Valli A, Todesco M, Mateos I, Puga MI, Rubio-Somoza I, Leyva A, Weigel D, Garcia JA, Paz-Ares J. 2007. Target mimicry provides a new mechanism for regulation of microRNA activity. *Nature Genetics* 39: 1033–1037.

Gao F, Wang K, Liu Y, Chen Y, Chen P, Shi Z, Luo J, Jiang D, Fan F, Zhu Y et al. 2015. Blocking miR396 increases rice yield by shaping inflorescence architecture. *Nature Plants* 2: 15196.

Gong R, Cao H, Zhang J, Xie K, Wang D, Yu S. 2018. Divergent functions of the GAGA-binding transcription factor family in rice. *The Plant Journal* 94: 32–47.

Hornitschek P, Kohnen MV, Lorrain S, Rougemont J, Ljung K, López-Vidriero I, Franco-Zorrilla JM, Solano R, Trevisan M, Pradervand S et al. 2012. Phytochrome interacting factors 4 and 5 control seedling growth in changing light conditions by directly controlling auxin signaling. *The Plant Journal* 71: 699–711.

Hornitschek P, Lorrain S, Zoete V, Michielin O, Fankhauser C. 2009. Inhibition of the shade avoidance response by formation of non-DNA binding bHLH heterodimers. *EMBO Journal* 28: 3893–3902.

Ikeda-Kawakatsu K, Yasuno N, Oikawa T, Iida S, Nagato Y, Maekawa M, Kyozuka J. 2009. Expression level of *ABERRANT PANICLE ORGANIZATION1* determines rice inflorescence form through control of cell proliferation in the meristem. *Plant Physiology* 150: 736–747.

Ji X, Du Y, Li F, Sun H, Zhang J, Li J, Peng T, Xin Z, Zhao Q. 2019. The basic helix-loop-helix transcription factor, OsPIL15, regulates grain size *via* directly targeting a purine permease gene *OsPUP7* in rice. *Plant Biotechnology Journal* 17: 1527–1537.

Jiao Y, Wang Y, Xue D, Wang J, Yan M, Liu G, Dong G, Zeng D, Lu Z, Zhu X et al. 2010. Regulation of *OsSPL14* by OsmiR156 defines ideal plant architecture in rice. *Nature Genetics* 42: 541–544.

de Jong RN, Truffault V, Diercks T, Ab E, Daniels MA, Kaptein R, Folkers GE. 2008. Structure and DNA binding of the human Rtf1 Plus3 domain. *Structure* 16: 149–159.

Kaiserli E, Páldi K, O'Donnell L, Batalov O, Pedmale UV, Nusinow DA, Kay SA, Chory J. 2015. Integration of light and photoperiodic signaling in transcriptional nuclear foci. *Developmental Cell* 35: 311–321.

Lee J, He K, Stolc V, Lee H, Figueroa P, Gao Y, Tongprasit W, Zhao H, Lee I, Deng XW. 2007. Analysis of transcription factor HY5 genomic binding sites revealed its hierarchical role in light regulation of development. *Plant Cell* **19**: 731–749.

Leivar P, Quail PH. 2011. PIFs: pivotal components in a cellular signaling hub. *Trends in Plant Science* **16**: 19–28.

Li M, Li H, Hu X, Pan X, Wu G. 2011. Genetic transformation and overexpression of a rice *Hd3a* induces early flowering in *Saussurea involucrata* Kar. et Kir. ex Maxim. *Plant Cell Tissue and Organ Culture* **106**: 363–371.

Liu Q, Han R, Wu K, Zhang J, Ye Y, Wang S, Chen J, Pan Y, Li Q, Xu X *et al.* 2018. G-protein βγ subunits determine grain size through interaction with MADS-domain transcription factors in rice. *Nature Communications* **9**: 852.

Loudet O, Michael TP, Burger BT, Le Metté C, Mockler TC, Weigel D, Chory J. 2008. A zinc knuckle protein that negatively controls morning-specific growth in *Arabidopsis thaliana*. *Proceedings of the National Academy of Sciences, USA* **105**: 17193–17198.

Ma Q, Dai X, Xu Y, Guo J, Liu Y, Chen N, Xiao J, Zhang D, Xu Z, Zhang X *et al.* 2009. Enhanced tolerance to chilling stress in *OsMYB3R-2* transgenic rice is mediated by alteration in cell cycle and ectopic expression of stress genes. *Plant Physiology* **150**: 244–256.

Martínez-García JF, Huq E, Quail PH. 2000. Direct targeting of light signals to a promoter element-bound transcription factor. *Science* **288**: 859–863.

Nakagawa T, Kurose T, Hino T, Tanaka K, Kawamukai M, Niwa Y, Toyooka K, Matsuoka K, Jinbo T, Kimura T. 2007. Development of series of gateway binary vectors, pGWBs, for realizing efficient construction of fusion genes for plant transformation. *Journal of bioscience and bioengineering* **104**: 34–41.

Nakamura Y, Kato T, Yamashino T, Murakami M, Mizuno T. 2007. Characterization of a set of phytochrome-interacting factor-like bHLH proteins in *Oryza sativa*. *Bioscience Biotechnology and Biochemistry* **71**: 1183–1191.

Oh E, Zhu JY, Wang ZY. 2012. Interaction between BZR1 and PIF4 integrates brassinosteroid and environmental responses. *Nature Cell Biology* **14**: 802–809.

Paik I, Kathare PK, Kim JI, Huq E. 2017. Expanding roles of PIFs in signal integration from multiple processes. *Molecular Plant* **10**: 1035–1046.

Qi Z, Xiong L. 2013. Characterization of a purine permease family gene *OsPUP7* involved in growth and development control in rice. *Journal of Integrative Plant Biology* **55**: 1119–1135.

Quint M, Delker C, Franklin KA, Wigge PA, Halliday KJ, van Zanten M. 2016. Molecular and genetic control of plant thermomorphogenesis. *Nature Plants* **2**: 15190.

Shor E, Paik I, Kangisser S, Green R, Huq E. 2017. PHYTOCHROME INTERACTING FACTORS mediate metabolic control of the circadian system in Arabidopsis. *New Phytologist* **215**: 217–228.

Si L, Chen J, Huang X, Gong H, Luo J, Hou Q, Zhou T, Lu T, Zhu J, Shangguan Y *et al.* 2016. *OsSPL13* controls grain size in cultivated rice. *Nature Genetics* **48**: 447–456.

Sun J, Qi L, Li Y, Chu J, Li C. 2012. PIF4-mediated activation of *YUCCA8* expression integrates temperature into the auxin pathway in regulating *Arabidopsis* hypocotyl growth. *PLoS Genetics* **8**: e1002594.

Sun J, Qi L, Li Y, Zhai Q, Li C. 2013. PIF4 and PIF5 transcription factors link blue light and auxin to regulate the phototropic response in *Arabidopsis*. *Plant Cell* **25**: 2102–2114.

Sun W, Xu XH, Wu X, Wang Y, Lu X, Sun H, Xie X. 2015. Genome-wide identification of microRNAs and their targets in wild type and *phyB* mutant provides a key link between microRNAs and the phyB-mediated light signaling pathway in rice. *Frontiers in Plant Science* **6**: 372.

Takano M, Inagaki N, Xie X, Yuzurihara N, Hihara F, Ishizuka T, Yano M, Nishimura M, Miyao A, Hirochika H *et al.* 2005. Distinct and cooperative functions of phytochromes A, B, and C in the control of deetiolation and flowering in rice. *Plant Cell* **17**: 3311–3325.

Terao T, Nagata K, Morino K, Hirose T. 2010. A gene controlling the number of primary rachis branches also controls the vascular bundle formation and hence is responsible to increase the harvest index and grain yield in rice. *Theoretical Applied Genetics* **120**: 875–893.

Toki S, Hara N, Ono K, Onodera H, Tagiri A, Oka S, Tanaka H. 2006. Early infection of scutellum tissue with *Agrobacterium* allows high-speed transformation of rice. *The Plant Journal* **47**: 969–976.

Wang S, Li S, Liu Q, Wu K, Zhang J, Wang S, Wang Y, Chen X, Zhang Y, Gao C *et al.* 2015. The OsSPL16-GW7 regulatory module determines grain shape and simultaneously improves rice yield and grain quality. *Nature Genetics* **47**: 949–954.

Wang S, Wu K, Yuan Q, Liu X, Liu Z, Lin X, Zeng R, Zhu H, Dong G, Qian Q *et al.* 2012. Control of grain size, shape and quality by OsSPL16 in rice. *Nature Genetics* **44**: 950–954.

Wier AD, Mayekar MK, Heroux A, Arndt KM, VanDemark AP. 2013. Structural basis for Spt5-mediated recruitment of the Paf1 complex to chromatin. *Proceedings of the National Academy of Sciences, USA* **110**: 17290–17295.

Xie C, Zhang G, An L, Chen X, Fang R. 2019. Phytochrome-interacting factor-like protein OsPIL15 integrates light and gravitropism to regulate tiller angle in rice. *Planta* **250**: 105–114.

Yamaguchi R, Nakamura M, Mochizuki N, Kay SA, Nagatani A. 1999. Light-dependent translocation of a phytochrome B-GFP fusion protein to the nucleusin transgenic *Arabidopsis*. *Journal of Cell Biology* **145**: 437–445.

Yue B, Xue WY, Luo LJ, Xing YZ. 2006. QTL Analysis for flag leaf characteristics and their relationship with yield and yield traits in rice. *Yi Chuan Xue Bao* **33**: 824–832.

Zhang JP, Yu Y, Feng YZ, Zhou YF, Zhang F, Yang YW, Lei MQ, Zhang YC, Chen YQ. 2017. MiR408 regulates grain yield and photosynthesis *via* a phytocyanin protein. *Plant Physiology* **175**: 1175–1185.

Zhang Y, Mayba O, Pfeiffer A, Shi H, Tepperman JM, Speed TP, Quail PH. 2013. A quartet of PIF bHLH factors provides a transcriptionally centered signaling hub that regulates seedling morphogenesis through differential expression-patterning of shared target genes in *Arabidopsis*. *PLoS Genetics* **9**: e1003244.

Zhang YC, Yu Y, Wang CY, Li ZY, Liu Q, Xu J, Liao JY, Wang XJ, Qu LH, Chen F *et al.* 2013. Overexpression of microRNA OsmiR397 improves rice yield by increasing grain size and promoting panicle branching. *Nature Biotechnology* **31**: 848–852.

Zhang YM, Yan YS, Wang LN, Yang K, Xiao N, Liu YF, Fu YP, Sun ZX, Fang RX, Chen XY. 2012. A novel rice gene, *NRR* responds to macronutrient deficiency and regulates root growth. *Moecular Plant* **5**: 63–72.

Zheng T, Yu H, Zhang H, Wu Z, Wang W, Tai S, Chi L, Ruan Y, Wei Z, Shi J *et al.* 2015. Rice functional genomics and breeding database (RFGB)-3K rice SNP and InDel sub-database. *Chinese Science Bulletin* **60**: 367–371.

Zhou J, Liu Q, Zhang F, Wang Y, Zhang S, Cheng H, Yan L, Li L, Chen F, Xie X. 2014. Overexpression of OsPIL15, a phytochrome-interacting factor-like protein gene, represses etiolated seedling growth in rice. *Journal of Integrative Plant Biology* **56**: 373–387.

Supporting Information

Additional Supporting Information may be found online in the Supporting Information section at the end of the article.

Fig. S1 Agronomic traits of OsmiR530-OE and target mimic (MIM530) lines.

Fig. S2 Comparison of the peduncle in miR530-OE, target mimic (MIM530) and WT plants.

Fig. S3 Expression of OsmiR530 and *OsPL3* in various rice tissues.

Fig. S4 Diagram of two sgRNAs targeting *OsPL3* in the rice genome.

Fig. S5 Analysis of the OsPL3 protein sequence in the WT and *OsPL3*-KO lines.

Fig. S6 Agronomic traits of *OsPL3*-KO lines.

Fig. S7 Diagram of two sgRNAs targeting *OsPIL15* in the rice genome.

Fig. S8 Analysis of the OsPIL15 protein sequence in the rice WT and *OsPIL15*-KO lines.

Fig. S9 Expression of OsmiR530 in rice *OsPIL15* transgenic lines.

Fig. S10 Alignment of mature miR530 sequences identified in miRBase.

Fig. S11 PHYB physically interacts with OsPIL15.

Fig. S12 Knockout of *PHYB* in rice results in smaller seed.

Table S1 Details regarding the primers and DNA fragments used in this study.

Please note: Wiley Blackwell are not responsible for the content or functionality of any Supporting Information supplied by the authors. Any queries (other than missing material) should be directed to the *New Phytologist* Central Office.